Agricultural and Forest Meteorology 249 (2018) 488–500

Contents lists available at ScienceDirect

Agricultural and Forest Meteorology

journal homepage: www.elsevier.com/locate/agrformet

The influence of hydrological variability on inherent water use efficiency in forests of contrasting composition, age, and precipitation regimes in the Pacific Northwest

Hyojung Kwon[a,*], Beverly E. Law[a], Christoph K. Thomas[b,c], Brittany G. Johnson[a]

[a] Department of Forest Ecosystems & Society, Oregon State University, Corvallis, OR 97331, USA
[b] College of Earth, Ocean & Atmospheric Sciences, Oregon State University, Corvallis, OR, USA
[c] Micrometeorology Group, University of Bayreuth, D-95440 Bayreuth, Germany

ARTICLE INFO

Keywords:
Water use efficiency
Drought
Climate and age gradients
Pacific Northwest

ABSTRACT

The Pacific Northwest (PNW) region of the United States has some of the most productive forests in the world. As precipitation regimes may shift with changing climate in this area, droughts are predicted to increase in both frequency and degree of severity, which will have a significant impact on already drought-prone ecosystems. When modeling ecosystem responses to drought, it is important to consider the physiology of individual tree species since the variations in drought sensitivity among species is easily overlooked when plants are characterized using broad plant functional types. Here we explore the use of inherent water-use efficiency as an index of drought sensitivity in semi-arid young and mature ponderosa pine forests and a mesic mature Douglas-fir forest in the PNW. Summer maximum of an evapotranspiration-based WUE (WUE_i) was 2.5 times higher in young and mature pines in semi-arid climate than Douglas-fir in mesic climate (12.2 and 11.3 versus 4.7 g C kPa per kg H_2O, respectively). In contrast, annually averaged WUE_i was similar among the sites (2.8 g C kPa per kg H_2O for pines and 2.4 g C kPa per kg H_2O for Douglas-fir). The effect of drought stress on WUE_i was most pronounced in young pine, followed by mature pine and Douglas-fir (32, 11, and 6% increase in WUE_i per % decline in soil water content, respectively) which reflect differences in age-related ecosystem structure (root system, stem capacitance, and soil water holding capacity). Among sites, the responses of WUE_i to climate variability were largely driven by changes in evapotranspiration (ET) compared to gross primary productivity (GPP). However, in areas where evaporation is the primary component of ET, such as the open canopy ponderosa forests of the PNW, the contribution of soil processes to ET can overshadow the reaction of vegetation transpiration (T) to changes in water availability. In these cases, utilizing a transpiration-based WUE (WUE_{i_T}) in vegetation models will yield a more accurate representation of plant activity during drought. These results highlight the importance of incorporating differences in species- and age-related WUE_i in models in diverse forest types at regional and global scales to improve predictions in ecosystem responses to climate change.

1. Introduction

Forest ecosystems are increasingly vulnerable to tree mortality as global climate change progresses (Allen et al., 2010; Williams et al., 2012). Rates of forest decline have particularly increased in regions where low levels of water availability are further exacerbated by a warming climate (Assal et al., 2016). Water limitations result in reductions in forest productivity (Jung et al., 2010; Thomas et al., 2009; Zha et al., 2010; Zhao and Running, 2010) and increases the susceptibility of trees to insects and disease (Meddens et al., 2012). This is of growing concern in the field of climate change research as the net global forest carbon sink lies primarily in temperate and boreal forests (Pan et al., 2011) which may be storing a large fraction (35% per year) of the carbon released from the consumption of fossil fuels (IPCC, 1995; Tans et al., 1990). While the relationship between water availability and forest productivity has been well established, the ability of process models to accurately predict the sensitivity of simulated carbon uptake to drought must be improved (Law et al., 2000; Leuzinger and Thomas, 2011; Zeppel et al., 2011).

Ecosystem-scale water use efficiency (WUE = GPP/ET; GPP is gross primary production and ET is evapotranspiration) is a key diagnostic parameter to examine the link between carbon and water cycles. The responses of WUE to fluctuating environmental conditions is often used to approximate the physiological adaptations of an ecosystem to a

* Corresponding author.
E-mail address: hyojung.kwon@oregonstate.edu (H. Kwon).

http://dx.doi.org/10.1016/j.agrformet.2017.08.006
Received 3 March 2017; Received in revised form 8 July 2017; Accepted 6 August 2017
Available online 18 August 2017
0168-1923/

changing climate (Beer et al., 2009; Keenan et al., 2013; Linderson et al., 2012; Lu and Zhuang, 2010; Tang et al., 2014). WUE is also effectively used as an indicator of ecosystem drought stress (Brümmer et al., 2012; Irvine et al., 2004; Thomas et al., 2009). Various models have addressed the interaction between carbon and water cycles using WUE, and bio-physiological processes have been incorporated in such models to quantify carbon and water fluxes simultaneously via estimations of stomatal regulation (Sellers et al., 1997; Sun et al., 2011; Tian et al., 2010). Assessments of model performance on simulating WUE are conducted by comparing flux measurements across plant functional types (PFTs; Schwalm et al., 2010; Tang et al., 2014). However, due to the limited availability of field observations in drought-prone ecosystems, the dynamics of WUE from models have rarely been validated in these climates (Williams et al., 2001). Better utilization of available data in drought-prone ecosystems will vastly improve our understanding of carbon and water coupling and the responses of these ecosystems to current and potential variations in climate (Schwalm et al., 2010).

There have been recent global synthesis efforts to assess spatial variability and trends of WUE across ecosystems (Beer et al., 2009; Huang et al., 2015; Jasechko et al., 2013; Keenan et al., 2013; Linderson et al., 2012; Tang et al., 2014). The concept of inherent WUE (WUE_i = GPP*VPD/ET; VPD is vapor pressure deficit), first proposed by Beer et al. (2009), utilizes the relationship between GPP and VPD to account for the confounding effect of VPD on the separation of GPP and ET responses to changes in climate. Using eddy flux data over 40 sites across a range of PFTs and climate conditions, Beer et al. (2009) reported the dynamic ranges of WUE_i. Although few sites were in dry regions, they observed an increase in WUE_i with short-duration moderate drought. Keenan et al. (2013) also showed a substantial upward trend in WUE_i in mesic temperate and boreal forests of the Northern Hemisphere over the past two decades using FLUXNET eddy covariance data from 21 sites, which was proposed to be the result of a strong CO_2 fertilization effect. Most of the global syntheses focus on the changes of WUE_i associated with different PFTs, but few examined WUE_i in regions that regularly experience drought, like the western USA.

Drought-prone semi-arid ecosystems comprise nearly 18% of the earth's land area (2.4 billion hectares) and have substantial carbon sequestration potential (Lal, 2004; Rotenberg and Yakir, 2010). There is a pressing need to scrutinize the response of WUE in water-limited environments where WUE is directly influenced by interannual variations in drought stress. In separate prior studies in the semi-arid forests of Oregon, we examined interannual variability in WUE or WUE_i in young and mature ponderosa pine forests and found that they generally increased as summer soil water deficit and VPD increased and were higher in more extreme drought years (Irvine et al., 2004; Ruehr et al., 2012; Thomas et al., 2009; Vickers et al., 2012). We found higher WUE in young than mature and old ponderosa pine (5, 3, and 4 g C m^{-2} mm^{-1}, respectively) when adjusted for leaf area index (LAI) differences (Irvine et al., 2004). Vickers et al. (2012) reported that WUE_i was ~70% larger in young pine (4 g C kPa per kg H_2O) than mature pine (2.6 g C kPa per kg H_2O) during the seasonal drought. This indicates that the younger trees are more susceptible to drought stress than the mature trees due to the higher relative sensitivity of canopy conductance to VPD and earlier water shortage during seasonal drought. WUE in mature ponderosa pine increased with drought stress during the growing season with no obvious differences between relatively dry or wet years (2002–2008), suggesting the mature ponderosa pine can adapt well to increasing drought stress (Thomas et al., 2009).

The aforementioned studies focused on ecosystem responses to drought stress by evaluating WUE or WUE_i, both of which are derived from measurements of ET, at ponderosa pines in semi-arid sites. However, one of the limitations of WUE_i, particularly in drought-prone open canopy forests, is that the responses of trees to water availability can be unclear since ET is dominated not by tree transpiration, but a combination of understory transpiration and evaporation from the forest floor during water-limited periods (Black and Kelliher, 1989). Throughout periods of drought, particularly in low LAI forests, WUE_{i_T} (derived from tree transpiration (T), GPP*VPD/T) can be a better representation of drought stress in trees can be.

This study includes further years of data in the young and mature ponderosa pine forests in addition to a new mesic site occupied by Douglas-fir, all of which experience seasonal drought. Our objectives were to: (1) determine the response of WUE_i and WUE_{i_T} to drought stress between mature evergreen needleleaf forests growing in mesic and dry climates (mature ponderosa pine *vs.* mature Douglas-fir) and differences among stand ages in semi-arid climate conditions (young *vs.* mature ponderosa pines) and (2) assess the feasibility of defining species- or age-specific WUE_i as a plant trait for improving models.

2. Materials and methods

2.1. Study sites

The study was conducted in mature and young ponderosa pine in the semi-arid climate of Central Oregon, while Douglas-fir is in the mesic ecoregion of Western Oregon. All sites are part of the AmeriFlux network (http://ameriflux.ornl.gov; Fig. A.1 in Supplementary materials). Both the mature and young ponderosa pine sites are within the network's Metolius site cluster that encompass a range of tree developmental stages since disturbance. The mature ponderosa pine forest (AmeriFlux site US-Me2, referred to hereafter as MP) is located east of the Cascade Range crest near Sisters, Oregon USA at an elevation of 1255 m (44.452N, 121.557W; Table 1). The mean stand age is 64 years with the oldest trees aged about 100 years. The overstory is almost exclusively composed of ponderosa pine (*Pinus ponderosa Dougl.* ex Laws) with a few scattered incense cedars (*Calocedrus decurrens* (Torr.) Florin) and has a summer maximum leaf area index (LAI) of 2.8

Table 1
Site characteristics at mature ponderosa pine (MP), young ponderosa pine (MP), and mature Douglas fir (DF) locations. Numbers in parenthesis indicate the measurement year.

Site	MP	YP	DF
Latitude (°N)	44.451	44.315	44.6465
Longitude (°W)	121.558	121.6078	123.5515
Elevation (m)	1255	1008	263
Mean age (years)	67 (2012)	18 (2004)	41 (2005)
Mean height (m)	17 (2011)	3.1 (2003)	25 (2005)
Density (trees ha^{-1})	325 (2006)	260 (2003)	414 (2006)
Diameter at breast height (cm)	32.3 (2011)	8.3 (2007)	32.1 (2006)
Biomass (g C m^{-2})			
Wood	6293 (2011)	205 (2003)	10036 (2009)
Foliage	535 (2011)	62 (2003)	833 (2009)
Maximum leaf area index	2.8 (2007)	1.8 (2008)	9.4 (2006)
Rooting depth (m)	1.5	0.5	1.0
Foliar C:N	57:1 (2001)	–	36:1 (2003)
Soil $C:N^+$	24:1[a] (2001)	–	22:1[a] (2005)
Soil depth (m)	1.5	0.5	1.0
Soil sand/silt/clay fraction (%)	sandy	loamy sand	silty clay loam
	0.0–0.2 m: 69/24/7	0.0–0.1 m: 80/17/3	0.0–0.2 m: 33/35/32
	0.2–0.5 m: 66/27/7	0.1–0.2 m: 80/17/3	0.2–0.5 m: 29/33/38
	0.5–1.0 m: 54/35/11	0.2–0.5 m: 80/17/3	0.5–1.0 m: 33/35/32
30-year mean[b] annual temperature (°C)	7.5	7.6	10.6
30-year mean[b] annual precipitation (mm)	536	500	1821

[a] Soil C:N ratio at MP and DF was averaged from the measurements at 0–20, 20–50, and 50–100 cm depths.
[b] The 30-year mean (1981–2010) was obtained from the PRISM Group at Oregon State University (http://prismmap.nacse.org/nn/).

(Table 1). Tree height is homogeneous at about 17 m and the mean tree density is 325 trees ha^{-1} (Irvine et al., 2008). The understory is sparse with LAI of 0.6 and primarily composed of bitterbrush (*Purshia tridentata* (Push) DC.) and greenleaf manzanita (*Arctostaphylos patula* Greene). Soils at the site are sandy and freely draining with a soil depth of approximately 1.5 m (Schwarz et al., 2004; Irvine et al., 2008).

The young ponderosa pine forest (AmeriFlux site US-Me3, referred to hereafter as YP) is a 16-year old ponderosa pine plantation at an elevation of 1005 m (44.3154N, 121.6078W; Table 1) and located ~16 km south of MP. The site was clear-cut, stripped of debris, tilled, and replanted with clonal trees in 1987. The overstory is composed of ponderosa pine (*Pinus ponderosa Dougl.* ex Laws), and the understory is primarily Idaho bunchgrass (~70% of the understory; *Festuca idahoensis*) and bitterbrush (*Purshia tridentate* (Push) DC.; ~20%; Vickers et al., 2012). The average canopy height of the trees is 3.3 m and tree density is 260 trees ha^{-1}. The seasonal maximum LAI was 1.8 in 2007. Approximately 22% of the maximum LAI is that of understory, and the bunchgrass senesces in June. Soils are a freely draining sandy loam derived from volcanic ash (soil depth < 1 m).

The Douglas-fir forest (AmeriFlux site US-MRf, referred to hereafter as DF) is located on the east side of the Coast Range of Oregon, USA at an elevation of 1005 m (44.646. N, 123.551.W). The average stand age is 58 years. The overstory is almost exclusively composed of Douglas-fir (*Pseudotsuga menziesii* (Mirb.) Franco) and the maximum LAI is 9.4 as of 2006 (Thomas et al., 2013). Tree height is homogeneous at ~34 m, and the mean stand density is 414 trees ha^{-1}. The understory is sparse and composed mainly of salal (*Gaultheria shallon*) with a plant height of up to 0.8 m. Soils at the site are silty clay loam, well drained, and highly fertile. Deeper soils with more organic matter and clay results in a larger soil water holding capacity compared to pine sites.

The general climate in the region is characterized by hot, dry summers and precipitation that primarily occurs in winter and spring as a combination of snow and rain. DF experiences milder winters with little snow such that the growing season is almost year-round, whereas MP and YP experience snow and long periods of freezing temperatures with less total annual precipitation. Data used in these analyses include 2003–2012 for mature ponderosa pine, 2005–2008 for young ponderosa pine, and 2007–2010 for mature Douglas-fir. The 30-year mean temperature and precipitation, which were calculated using data from the Parameter–Elevation Regressions on Independent Slopes Model (PRISM Climate Group, Oregon State University, http://prism.oregonstate.edu, 1981–2010), were 7.5 °C and 536 mm at MP, 7.6 °C and 500 mm at YP, and 10.6 °C and 1821 mm at DF (Table 1).

2.2. Eddy covariance and meteorological measurements

Eddy-covariance (EC) measurements at MP were conducted using a three-dimensional sonic anemometer (model CSAT3, Campbell Scientific Inc., Logan, UT, USA) and an open-path infrared gas analyzer (model LI-7500, LI-COR Inc., Lincoln, NE, USA) at a height of 33.0 m. Meteorological measurements include net radiation (model CNR1, Kipp & Zonen, Delft, The Netherlands), photosynthetic active radiation (model PARlite, Kipp & Zonen), air temperature and relative humidity (model HMP45, Vaisala, Helsinki, Finland), and precipitation (model TE525WS, Texas Electronics, Dallas, TX, USA). Atmospheric CO_2 concentration was measured at multiple heights (0.3, 1.3, 6.0, 10.0, 20.0, 33.5, and 37.5 m) using a profile system equipped with a LI-820 gas analyzer to estimate CO_2 storage following quality control. LAI was measured using a LAI-2000 (LI-COR Inc.) and is reported as hemi-surface area. These data were corrected for clumping and include understory. Soil measurements include soil water content at 0–30 cm depth in 3 locations (model CS615, Campbell Scientific Inc.) and soil temperature at multiple depths (i.e., 2.0, 4.0, 8.0, 16.0, 32.0, and 64.0 cm) using Type-T thermocouples (see Thomas et al. (2009) and Vickers et al. (2012) for more information).

Instrumentation at YP and DF is similar to MP. The EC measurement height is 12.0 m at YP and 38.0 m at DF, and a closed-path IRGA (model LI-7000, LI-COR Inc.) was deployed at DF due to the relatively higher frequency of rain at that site causing interference with an open-path sensor. The CO_2 concentration of the profile system was conducted at 1.0, 5.0, and 12.0 m at YP and 0.5, 1.7, 4.0, 9.0, 18.0, 27.0, and 37.9 m at DF (see Vickers et al. (2012) and Thomas et al. (2013) for more information).

Processing of raw data (10 or 20 Hz) to produce 30-min flux data at MP and DF followed Thomas et al. (2009). In brief, it includes outlier removal of turbulent variables in raw data, post-hoc density correction for CO_2 and H_2O fluxes (Webb et al., 1980), and rigorous quality control of initial 30-min flux data using a combination of higher-order statistics and quality flags for stationarity (Foken and Wichura, 1996) and turbulence development (Thomas and Foken, 2002). After removing unsatisfactory flagged data, gap-filling was conducted separately for CO_2 and H_2O fluxes. The flux data were gap-filled using linear interpolation when data gaps were less than two hours. When the data gaps were greater than two hours, a light response model and temperature response model were applied to the daytime and the nighttime data separately corresponding to different temperature and soil water content (SWC) classes. H_2O flux data were categorized with different SWC intervals and gap-filled using the Priestley-Taylor model (see Appendix A in Thomas et al. (2009)). EC measurements were conducted to measure ET from understory at MP. The instrumental setup and data recording and processing of the subcanopy EC system were identical to the one above the canopy.

For YP, the initial raw data quality control and calculation of 30-min flux data was identical to that of the other two sites. However, a u_*-filter was applied to nighttime fluxes in turbulent mixing strength. At YP, the critical value of u_* was 0.1 m s^{-1} which represents the smallest class value of u_* with a flux class mean that is greater than or equal to 95% of the average fluxes for all larger u_* classes (Vickers et al., 2012). Short gaps in daytime flux were filled using the mean diurnal variation method (Falge et al., 2001) with window sizes of 5 days followed by 9 days. The remaining gaps were filled using the multi-year averaged data for a given 30-min period. Like for MP, gaps in nighttime CO_2 flux were filled using the temperature response model. In order to reflect seasonal changes in temperature and SWC and to have a sufficient number of data points, the model ran over 45-day periods (Vickers et al., 2012).

The recently published FLUXNET2015 data (http://fluxnet.fluxdata.org/data/fluxnet2015-dataset/), which contains GPP calculated from daytime temperature-corrected ecosystem respiration (RE), overlaps with only the data at the MP site, which used nighttime temperature-corrected RE to determine GPP values. We applied a Kruskal-Wallis test to assess differences in the means of GPP between the data used in this study and those from FLUXNET2015. Because the means of GPP were not significantly different between methods except in 2003 and 2006 (Table A.1 in Supplementary materials), we used GPP corrected with nighttime-temperature in order to keep the data processing consistent among sites in the study.

2.3. Sap flow measurements and transpiration

Sap flux was measured by the heat dissipation technique (Granier, 1987) between April and November over a 10-year period at MP (2003–2012) and a 4-year period at DF (2006–2009). A detailed description of our sap flow measurement methods can be found in Irvine et al. (2002). In brief, sap flux sensors were installed across a range of tree sizes (diameter at breast height (DBH) from 22 to 41 cm in 12 trees at MP and from 29 to 48 cm in 10 trees at DF) based on a stand surveys to investigate variation in sap flux in relation to tree size and to accurately scale stand-level T. The selected trees were within the tower footprint at both sites. Sap flow was measured over the outer 20 mm of sapwood and recorded as a 10-min average of one-minute measurements (model CR10X, Campbell Scientific Inc.). Sap velocity was

calculated empirically from probe temperature differentials (Granier, 1987) and zero flow was estimated at night when VPD ≤ 0.3 kPa. We also accounted for the proportion of sapwood area at different sapwood depths and the decline in sap velocity with sapwood depth when calculating tree transpiration. To measure the change in sap velocity with depth, in addition to the 20 mm sap flux probe, three 10-mm probes were installed at different sapwood depths in four trees at both the MP and DF sites. The decline in sap velocity with depth was calculated from mean daily sap fluxes from the profiles expressed relative to the sap flux over the 0–20 mm sapwood depth.

Transpiration was estimated based on mean sap flux for each tree, the proportion of sapwood area at different sapwood depths, and the decline in sap flux with sapwood depth. The naturally occurring temperature gradient between the heater and reference probe is often a sizable source of error in sap flux measurement. This temperature gradient was assessed at the 0–20 mm sapwood depth in all trees. Errors associated with temperature gradients were 12% overestimation of mean daily sap flux at MP and DF and were corrected accordingly. In order to compare T and ET at the stand level, we scaled T by multiplying mean sap flux by sapwood-to-ground area ratio, derived from four inventory plots (each with a 15 m radius) located within the footprint of the EC system (see Irvine et al. (2002, 2004) for more detailed information).

At YP, sap flux was not measured during the EC measurement period. However, a similar young ponderosa pine site was established in 2010 (Ameriflux site US-Me6) and is located approximately 850 m north of YP. Both sites were re-forested in the early 1990s and had similarly aged ponderosa pines. At US-Me6, sap flux measurements were conducted for four trees from May through October in 2010 and 2011, using the methods described above (Ruehr et al., 2012). Errors associated with temperature gradients were 7% overestimation at YP and were corrected accordingly. Sapwood-to-ground area ratio for stand-level T was derived from tree inventories of 4 × 17 m radius plots. Given the fact that both sites contain the same species of similar age and are in close proximity to one another, we assumed a similar monthly ratio of T to ET between the two sites. We applied the ratio of T/ET at US-Me6 to estimate T at YP. We used YP as the site of interest to represent a young ponderosa pine because YP had more years of overlapping measurements with MP and DF than US-Me6.

2.4. Ecosystem processes and drivers

To diagnostically interpret the dependency of WUE_i on vegetation type and environmental conditions, canopy conductance (G_c) was calculated by rearranging the Penman-Monteith equation as follows:

$$G_c = \left\{ \frac{\rho c_p VPD}{\gamma \lambda E} + \frac{1}{g_a}\left[\frac{\Delta}{\gamma}\left(\frac{R_n - G}{\lambda E} - 1 \right) - 1 \right] \right\}^{-1} \quad (1)$$

where Δ is the slope of saturation vapor pressure curve (kPa K^{-1}); λ is the psychrometric constant (kPa K^{-1}); E is evaporation; ρ is air density (kg m^{-3}); c_p is the specific heat of air (MJ kg^{-1} K^{-1}); R_n is net radiation (W m^{-2}); G is ground heat flux (W m^{-2}); VPD is vapor pressure deficit (kPa); and g_a is the aerodynamic conductance (m s^{-1}). Levels of g_a are estimated as:

$$g_a = \frac{1}{r_a} = \frac{1}{r_{am} + r_b} \quad (2a)$$

$$r_{am} = \frac{\overline{U}}{{u_*}^2} \quad (2b)$$

$$r_b = \left(\frac{2}{k u_*}\right)\left(\frac{K}{D_v}\right)^{\frac{2}{3}} \approx \frac{4.626}{u_*} \quad (2c)$$

where r_a is the aerodynamic resistance (s m^{-1}) which consists of the aerodynamic resistance of momentum transfer (r_{am}) and the excess resistance (r_b; Thom, 1972; Kim and Verma, 1990); $\overline{U}$ is mean horizontal wind speed at a height; u_* is the friction velocity; κ is the Karman's constant; K is the thermal diffusivity; and D_v is the molecular diffusivity of water vapor. Stomatal conductance at canopy-level (g_s) was calculated by substituting T from sap flow measurements for λE in Eq. (1).

We computed a monthly time series of standardized precipitation evapotranspiration indices (SPEI) as a site-specific drought indicator (Vicente-Serrano et al., 2013, 2010). SPEI is calculated as a function of D (the difference between precipitation and potential ET, ET_p), and then aggregated at different time scales to represent the cumulative water balance over the previous number of months as follows:

$$D_n^k = \sum_{i=0}^{k-1} (P_{n-i} - ET_{p_{n-i}}) \quad n \geq k \quad (3)$$

where k (in months) is the timescale of aggregation and n is the calculation number. We used the SPEI package (Beguería and Vicente-Serrano, 2013) in R (R Core Team, 2016) and a 6-month integration period (k) to calculate SPEI. We estimated ET_p using the following equation:

$$ET_p = \alpha_{PT} \frac{\Delta R_n}{\rho(\Delta + \gamma)} \quad (4)$$

where α_{PT} is the Priestly-Taylor coefficient (=1.26; Priestley and Taylor, 1972). A positive SPEI indicates wet conditions, whereas negative SPEI indicates dry conditions.

Half-hourly values of WUE_i were calculated during the daytime (defined as when PAR exceeded 150 μmol m^{-2} s^{-1}). WUE_i was derived from ET, which was converted from λE (latent heat flux, W m^{-2}). To calculate WUE_{i_T}, levels of T were normalized by LAI to determine stress per unit leaf area. In order to dampen the influence of precipitation on WUE_i and WUE_{i_T}, we excluded data both during and for 6 h after precipitation events. In addition, the pumice was permeable at the sites, leading to a very quick percolation after precipitation. The top soil layer was never saturated and this minimized bare soil evaporation. In order to focus on flux dynamics in response to drought, we calculated a relative fraction of each variable as the ratio of the values under non-limited soil water conditions (pre-drought) to those under limited soil water condition (drought). For the analysis, we selected data (PAR > 500 μmol m^{-2} s^{-1}) for the non-limited soil condition with the highest plant activity from DOY 157–166 for MP and YP and DOY 166–175 for DF.

Pronounced seasonality in water availability results in dynamic ecosystem carbon and water cycles at the sites. To examine ecologically meaningful events associated with the site hydrology, we present annual variations in precipitation and WUE_i based on the water year (1 October–30 September). We used anomalies in precipitation intensity and annual precipitation amount to define dry, normal, and wet years (U.S. Geological Survey, 1991). Precipitation intensity was calculated as annual precipitation divided by total number of precipitation days per year. Anomalies were defined as deviates from the mean precipitation intensity and annual precipitation during the measurement years. We defined a year as “dry” when both intensity and amount were below the normal values (i.e. negative) in a given year and “wet” when both parameters were greater than the normal values (i.e. positive). This analysis was applied only to MP where interannual variability of WUE_i can be assessed due to the length of the measurement period.

2.5. Statistical analyses

Subset regression analysis was employed to determine explanatory variables of variation in WUE_i using R package leaps (Lumley, 2017). The analysis assessed all possible models using a specified set of variables. The variables that best satisfied model-fitting criterion were identified based on Bayesian information criterion (BIC). We calculated Δ_i(BIC) (=BIC_i − BIC_{min}) and applied a weight method to quantify the

relative importance of each variable (Burnham and Anderson, 1998). The weight of each model was calculated as follows:

$$w_i(BIC) = \frac{\exp\left(-\frac{1}{2}\Delta_i(BIC)\right)}{\sum_{K=1}^{K}\exp\left(-\frac{1}{2}\Delta_k(BIC)\right)} \quad (5)$$

where Δ_i(BIC) is the distance from various models to the best model (in this case, the smallest BIC). If the sum of $w_i(BIC)$ of a variable is larger, relative to other variables, then the variable was regarded to be more important. We considered only linear models for the subset models and used data from those months which played a dominant role in seasonal variation of WUE_i (May–October) for each year in the analysis. We selected air temperature (T_{air}), soil water content (SWC), water balance (P-ET), and shortwave radiation (R_g) as explanatory variables. We used water balance as one of the water-related drivers as it is more critical than precipitation for plant physiological processes.

To assess differences among means of the annual WUE_i, we conducted Tukey-Kramer pairwise multiple comparison tests (Matlab Version 8.2.0.701 (R2013b), The MathWorks Inc., Natick, MA, 2013). Prior to the Tukey-Kramer comparison, we conducted Kruskal-Wallis ANOVA function test. When the null hypothesis, which states that all means are equal, was rejected, we proceeded with the Tukey-Kramer multiple comparison tests. This procedure conducted pairwise testing of means in a one-way analysis of variance with unequal sample sizes and a single critical difference, estimated from the Studentized range statistic, is calculated for each pair of means. Results were deemed significant when tolerance (α) was less than 0.05.

3. Results

3.1. Environmental conditions

Despite the short distance between MP and YP, the proximity of MP to the Cascade Range yielded in 45% higher annual precipitation than YP during the overlap measurement years (2005–2009, average of 514 and 353 mm y^{-1} at MP and YP, respectively). MP was 10% cooler than YP due to the 250-m elevation difference between the two sites (average of 7.5 and 8.2 °C; Table 2). Due to the influence of an oceanic climate, DF in the Coast Range was much wetter (averaged 1437 mm y^{-1} for overlap years of 2007–2008) and experienced warmer winters and cooler summers than MP and YP (Fig. A.2 in Supplementary materials).

Precipitation predominantly occurred from December to April (53–65% of the annual precipitation) at all sites, whereas dry months usually lasted from July to September (7–15%). Corresponding with the seasonal variation in precipitation, SWC reached its seasonal maximum of 40% at MP and DF and 20% at YP during the wet months, whereas the minimum SWC (10% at MP, 6% at YP, and 20% at DF) occurred during the dry months. Lower precipitation, higher soil porosity, and a thin organic layer at YP resulted in a more rapid decline and lower SWC than at MP. Higher SWC at DF was associated with higher precipitation and deeper organic soils allowing a higher soil water holding capacity. In addition, DF had ~50% lower monthly VPD during summers than MP and YP.

The measurement period for MP spanned a range of climate conditions including severe drought (2003–2005) during which time it received only 40–70% of the 30-year normal precipitation as well as anomalous wet years (2009–2012) when 104–110% of normal precipitation fell (Table 2). Within each drought year, a more negative SPEI clearly coincided with intensive and extended drought episodes (e.g., > 5 consecutive months, May–September) (Fig. A.3 in Supplementary materials). During wet years, SPEI was mostly positive. At YP and DF, which experienced primarily normal precipitation years during their respective measurement periods, there were continuous alterations between dry (SPEI < 0) and wet (SPEI > 0) periods within each year. SPEI was more negative at YP than at MP during the overlapping years, indicating that a higher degree of drought stress occurred at YP. The mean annual water balance ($P - ET$) for the water year was −39, −40, and 965 mm at MP, YP, and DF for overlap years of 2007–2008.

3.2. Seasonal variations in WUE_i and WUE_{i_T}

Monthly WUE_i showed similar seasonal patterns at all sites, reaching a maximum in late summer when seasonal precipitation was

Table 2
Annual meteorological conditions (P: precipitation; T_{air}: air temperature; VPD: vapor pressure deficit; SWC: soil water content), annual fluxes (NEE: net ecosystem CO_2 exchange; RE: ecosystem respiration; GPP: gross primary production; ET: evapotranspiration; T: transpiration), inherent water use efficiency (WUE_i) derived from ET, and inherent water use efficiency (WUE_{i_T}) derived from T, based on water year (Oct. 1 to Sep. 31) at mature ponderosa pine (MP), young ponderosa pine (MP), and mature Douglas fir (DF) sites. Numbers in parenthesis indicate a range (minimum to maximum) of monthly values of T_{air}, VPD, WUE_i, and WUE_{i_T} for each year.

Site	Year	P	T_{air}	VPD	SWC	NEE	RE	GPP	ET	T[a]	WUE_i	WUE_{i_T}[a]
MP	2003	271	7.9 (−1.7 to 22.1)	0.8 (0.1–2.1)	20.8	−248	1033	1281	410	71	3.5 (0.7–8.4)	8.6 (2.1–14.4)
	2004	213	7.7 (−0.8 to 19.6)	0.7 (0.1–1.7)	23.5	−467	1256	1724	535	107	2.9 (0.4–5.7)	3.8 (2.0–4.5)
	2005	325	7.8 (0.2–20.1)	0.7 (0.2–1.9)	21.0	−506	1136	1641	431	74	3.7 (1.7–11.3)	9.0 (1.9–15.4)
	2006	727	7.3 (−1.8 to 19.5)	0.6 (0.2–1.6)	24.8	−453	1038	1492	532	108	2.7 (0.6–8.7)	5.5 (1.8–8.8)
	2007	528	7.5 (−1.6 to 18.4)	0.7 (0.2–1.9)	21.1	−549	1151	1701	482	83	3.2 (0.7–7.5)	8.6 (2.0–16.1)
	2008	431	6.8 (−2.5 to 17.8)	0.7 (0.1–1.6)	23.8	−571	1156	1727	556	115	2.7 (0.3–5.1)	5.8 (1.9–13.1)
	2009	553	7.9 (−2.1 to 21.2)	0.8 (0.2–2.0)	20.7	−407	1193	1601	618	119	2.8 (0.8–7.2)	5.6 (1.7–11.4)
	2010	586	6.6 (−3.2 to 19.4)	0.6 (0.1–1.7)	22.4	−395	1264	1659	634	120	2.1 (0.5–5.5)	4.7 (1.5–7.7)
	2011	572	6.6 (−1.1 to 18.6)	0.6 (0.1–1.5)	18.9	−516	1137	1653	651	136	2.0 (0.4–4.8)	3.2 (1.5–5.6)
	2012	556	7.4 (−0.7 to 19.3)	0.7 (0.2–1.8)	20.3	−402	1428	1830	687	98	2.8 (0.5–10.5)	7.0 (2.3–10.4)
	Mean	476	7.4	0.7	21.7	−452	1179	1631	554	102	2.8	6.2
YP	2005	324	8.6 (0.1–20.5)	0.8 (0.2–2.2)	12.2	−19	656	684	356	42	2.3 (0.4–4.5)	7.8 (3.7–11.4)
	2006	485	8.1 (−2.3 to 20.7)	0.8 (0.2–2.1)	13.2	−118	702	822	342	39	3.6 (0.4–12.2)	17.2 (5.4–26.2)
	2007	291	8.3 (−1.5 to 20.0)	0.8 (0.2–1.7)	10.4	−79	671	752	352	35	2.6 (0.6–7.4)	10.1 (7.5–14.4)
	2008	390	7.5 (−2.2 to 18.9)	0.8 (0.2–1.9)	13.0	−160	662	827	408	44	2.6 (0.5–5.9)	12.8 (4.4–23.0)
	Mean	373	8.1	0.8	12.2	−94	673	771	364	40	2.8	12.0
DF	2007	1486	9.5 (2.9–16.4)	0.4 (0.1–0.7)	28.0	−601	2013	2614	521	115	2.4 (0.7–3.5)	1.2 (0.9–1.7)
	2008	1387	8.6 (1.9–16.0)	0.4 (0.1–1.1)	28.5	−489	2041	2530	421	100	2.5 (1.2-4.7)	1.2 (1.0–1.6)
	2009	1157	9.4 (2.8–17.3)	0.4 (0.1–1.0)	29.8	−313	2306	2620	448	99	2.7 (1.1–6.2)	2.1 (1.5–4.5)
	2010	1406	9.3 (1.7–15.4)	0.4 (0.1–0.9)	30.6	−360	2237	2598	404	–	2.7 (1.9–5.6)	–
	Mean	1359	9.0	0.4	29.7	−429	2149	2590	449	105	2.4	1.4

Units of variables: P (mm); T_{air} (°C); VPD (kPa); SWC (%); NEE, RE, and GPP (g C m^{-2} yr^{-1}); ET and T (mm); WUE_i and WUE_{i_T} (g C kPa per kg H_2O).

[a] Annual values of T and WUE_{i_T} were calculated from June to September, which was a common period of the sap flux measurements at all sites.

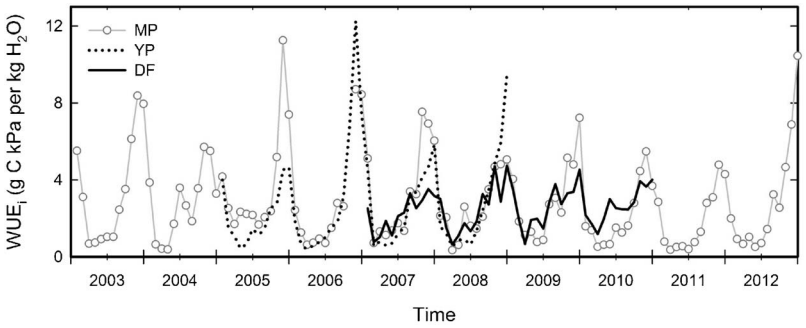

Fig. 1. Seasonal variation in monthly inherent water use efficiency (WUE_i) at mature ponderosa pine (MP), young ponderosa pine (YP), and mature Douglas-fir (DF) sites.

lowest but the seasonal variations in WUE_i were much larger at the pine sites than Douglas-fir (Fig. 1, Table 2). Values of WUE_i ranged from 0.4 to 12.2 g C kPa per kg H_2O at YP and 0.3 to 11.3 g C kPa per kg H_2O at MP over the entire measurement period for each site. WUE_i was higher at YP than MP when site-specific drought was more severe at YP (summers of 2006 and 2008) (Fig. A.3 in Supplementary materials). Outside of the seasonal drought period, MP and YP had similar monthly WUE_i, suggesting a species-specific WUE_i under non-water limiting conditions (Vickers et al., 2012). Although monthly WUE_i was higher at the pine sites than Douglas-fir in summer, the minimum WUE_i at the Douglas-fir site (0.7 g C kPa per kg H_2O) was roughly twice that of the pine while the maximum Douglas-fir WUE_i (6.2 g C kPa per kg H_2O) was less than half that of the pine sites (Table 2). Despite seasonal variations in WUE_i among years and sites, annual average WUE_i was similar across sites with values of 2.8 ± 0.6 g C kPa per kg H_2O for MP and YP and 2.4 ± 0.2 g C kPa per kg H_2O for DF.

The range in monthly values of WUE_{i_T} was greater in ponderosa pine (3.7–26.2 g C kPa per kg H_2O at YP and 1.5–16.1 g C kPa per kg H_2O at MP) than Douglas-fir (0.9–4.5 g C kPa per kg H_2O; Table 2). Unlike patterns in WUE_i, values of annual WUE_{i_T} varied by both species and age and were highest in YP, followed by MP and DF (12.0, 6.2, and 1.4 g C kPa per kg H_2O, respectively). Levels of annual WUE_{i_T} were greater than WUE_i by ~430% at YP and ~220% at MP, whereas WUE_{i_T} was only 58% of WUE_i at DF.

In order to examine the influence of physiological differences in species and age on WUE_{i_T}, we compared GPP, T and WUE_{i_T} (all normalized per unit leaf area; Fig. 2). Normalized GPP, T, and WUE_{i_T} were averaged from June to September of 2007–2009, during which T was available at all sites. In ponderosa pine, WUE_{i_T} increased substantially as summer soil water deficit increased, but showed almost no changes in Douglas-fir. The seasonal variation in normalized GPP and T was much larger at the two pine sites than at Douglas-fir. Compared to the maxima in June, normalized GPP and T were reduced by 40 and 80% in September at MP, 70 and 80% at YP, and 21 and 26% in DF. Higher rates of decline suggest more seasonal drought water stress in ponderosa pine than in Douglas-fir. The effect of drought stress on normalized GPP, T, and WUE_{i_T} was more pronounced in YP than MP.

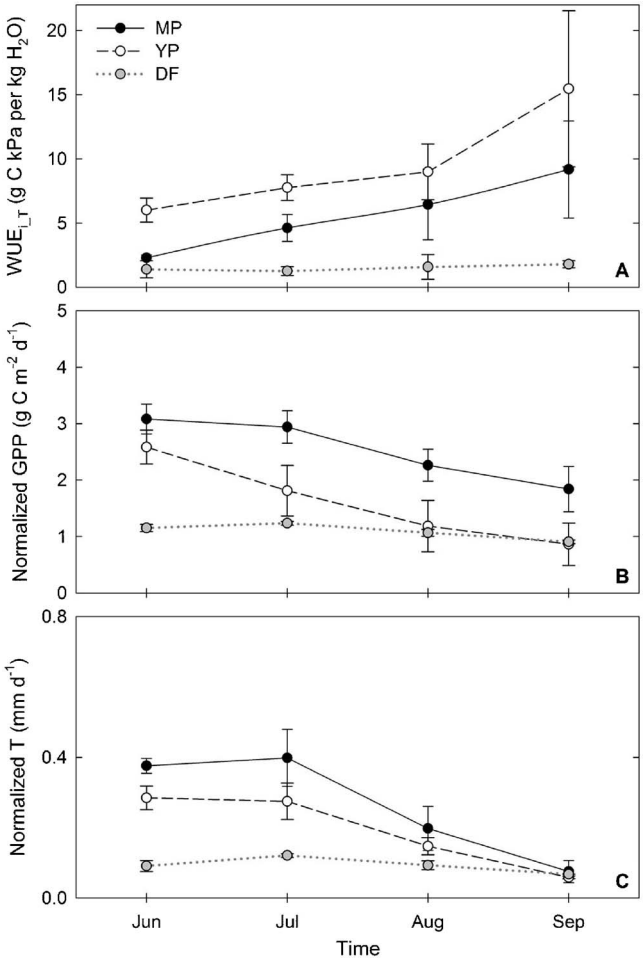

Fig. 2. Seasonal variation in monthly inherent water use efficiency (WUE_{i_T}) calculated with transpiration and the normalized gross primary production (GPP) and transpiration (T) at mature ponderosa pine (MP), young ponderosa pine (YP), and mature Douglas-fir (DF) sites. All variables were normalized per unit leaf area.

3.3. Explanatory variables of WUE_i and WUE_{i_T}

Environmental drivers of WUE_i varied between sites. The most important drivers of WUE_i at MP were T_{air}, SWC, P-ET, and R_g, whereas SWC was substantially more important than other variables at YP (Table A.2 in Supplementary materials). At DF, T_{air} was more important than water-related drivers. Given the close correlation between T_{air} and VPD ($Y = 0.205e^{0.12X}$, $R^2 = 0.92$ at MP, and $Y = 0.08e^{0.15X}$, $R^2 = 0.77$ at DF, where $X = T_{air}$ and $Y = VPD$), the dependence of WUE_i on T_{air} infers that VPD actually governs patterns of WUE_i.

To explore ecosystem responses to VPD, we examined the trends in WUE_i and WUE_{i_T} with varying VPD under both limited and non-limited soil water conditions (Fig. 3). When soil water was not a limiting factor, WUE_i increased with VPD at all sites. The rate of increase was similar at the two pine sites but steeper at the Douglas-fir site, indicating a higher sensitivity of WUE_i to changes in VPD at the Douglas-fir site. The responsiveness of WUE_i to changes in VPD under limited soil water conditions increased markedly at MP and YP at low to medium values of VPD, but tended to level off or even decrease as VPD continued to increase. At DF, however, the rate of WUE_i response to changes in VPD under water-limited conditions seemed to be less affected by levels of SWC, showing patterns that were similar to those of a non-water limited system.

The responses of WUE_{i_T} to changes in VPD were very similar to those of WUE_i, showing substantial increases of WUE_{i_T} at the two pine sites and almost no change of WUE_{i_T} at the Douglas-fir when soil water

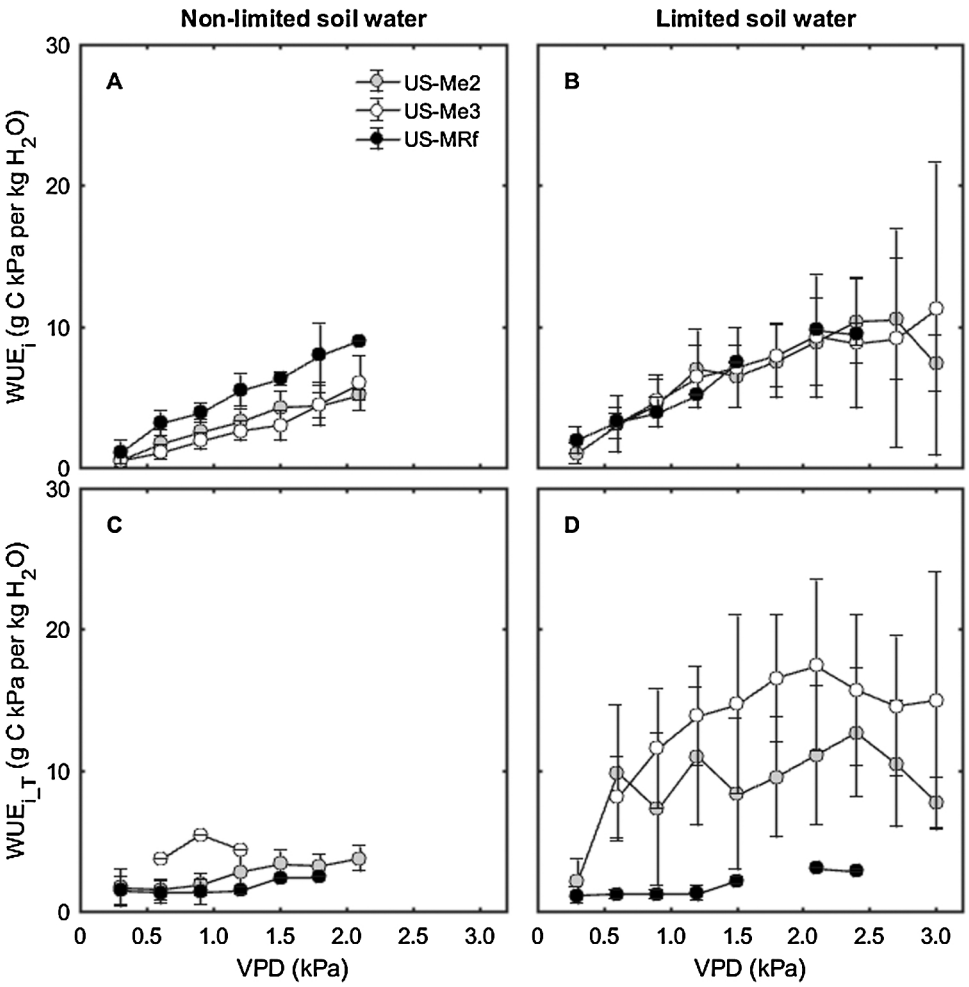

Fig. 3. Relationships between vapor pressure deficit (VPD) and inherent water use efficiency (WUE_i) calculated with evapotranspiration (ET) (panels A and B) and between VPD and inherent water use efficiency (WUE_{i_T}) calculated with transpiration (T) (panels C and D) under non-limited and limited soil water conditions at mature ponderosa pine (MP), young ponderosa pine (YP), and mature Douglas-fir (DF) sites. WUE_i and WUE_{i_T} were binned every 0.3 kPa VPD using half-hourly daytime data (PAR > 500 μmol m^{-2} s^{-1}). Data for non-limited soil water conditions were selected when the standardized precipitation evapotranspiration index (SPEI) > 0 and soil water content (SWC) > SWC_{ave} at each site, whereas criteria defining limited soil water were when SPEI < 0 and SWC < SWC_{min}. SWC_{ave} and SWC_{min} were 22 and 10% at MP, 12 and 6% at YP, and 29 and 20% at DF. Error bars indicate standard errors.

shifted from non-limited to limited conditions. Unlike the similar response of WUE_i to VPD at the two pines under water-limited conditions, a higher sensitivity of WUE_{i_T} to VPD was observed in young pine than mature pine. These results suggest that reduced SWC enhanced the influence of VPD on WUE_i and WUE_{i_T} at MP and YP but not at DF.

To more closely examine the relationships between WUE_i and SWC and between WUE_{i_T} and SWC, we compared trends in WUE_i and WUE_{i_T} during drought and non-drought conditions (expressed as a relative fraction and changes in SWC; Fig. 4). As SWC declined during the summer, WUE_i increased by 3.2 times at MP, 3.5 times at YP, and 1.5 times at DF compared non-drought conditions (Fig. 4A–C). For each percent decrease in SWC, WUE_i increased by 11% at MP, 32% at YP, and 4% at DF relative to pre-drought conditions (Fig. 4D). The rates of WUE_i increase in response to declining SWC were greater in ponderosa pines than in Douglas-fir, confirming that SWC was a more important driver of WUE_i in the more water-limited pine forests compared to the mesic Douglas-fir forest (Table A.2 in Supplementary materials & Fig. 4). As SWC approached minimum values, the relative fraction of ET was more sensitive to changing SWC than that of GPP at all sites (Fig. 4A–C). In order to examine plant response to SWC, the responses of WUE_{i_T} to SWC were also tested. The results were very similar to those of WUE_i, with the largest rates of change of WUE_{i_T} in young pine, followed by mature pine and Douglas-fir (12, 27, and 9% increases in WUE_{i_T} per% decline in SWC at MP, YP, and DF, respectively; Fig. 4E–H).

The increases in WUE_i and WUE_{i_T} in response to changes in SWC were strongly associated with the decreases in conductivity (G_c for WUE_i and g_s for WUE_{i_T}). Compared to G_c and g_s observed during non-drought conditions, G_c was reduced by 69% in mature pine, 76% in young pine, and 10% in Douglas-fir when SWC reached its minimum (10% at US-Me2, 6% at US-Me3, and 20% at US-MRf; Fig. 5A). Levels of g_s were lowered by 78% in mature pine, 73% in young pine, and 27% in Douglas-fir (Fig. 5B). Young pine had the lowest G_c (1.3 mm s^{-1}) and g_s (0.3 mm s^{-1}), which were ~45% of mature pine and ~20% of Douglas-fir.

3.4. Interannual variation of WUE_i at the mature pine site

Interannual variability of WUE_i was examined only at the MP site due to the length of the measurement period. WUE_i was highly dependent on amounts of precipitation, showing higher annual means (3.7 g C kPa per kg H_2O) during drought years (2003–2005) and lower (2.0 g C kPa per kg H_2O) during wet years (2010–2011, $p < 0.001$, Fig. 6A). Degrees of the identified drought and wet years were within the range of the 30-year time window (1981–2010; data not shown). The drought in 2003 corresponded with the lowest annual mean GPP, which significantly differed from GPP in the other years (Fig. 6B). However, the annual means of GPP in other drought years (2004 and 2005) were similar to those among non-drought years. The annual sum of GPP was 30% lower in 2003 compared to the measurement period maximum observed in 2012 (1830 g C m^{-2} yr^{-1}) but < 10% lower than GPP in the drought years of 2004 and 2005 (Table 2). The annual mean of ET in drought years was significantly lower than in wet years (Fig. 6C). The interannual daily mean of ET gradually increased from 1.1 to 1.9 mm d^{-1} (410.0–686.5 mm of annual ET) as drought stress was relieved by increasing annual amounts of precipitation.

The difference between annual WUE_i and the average WUE_i over the measurement period (WUE_i anomaly, ΔWUE_i) at MP decreased by

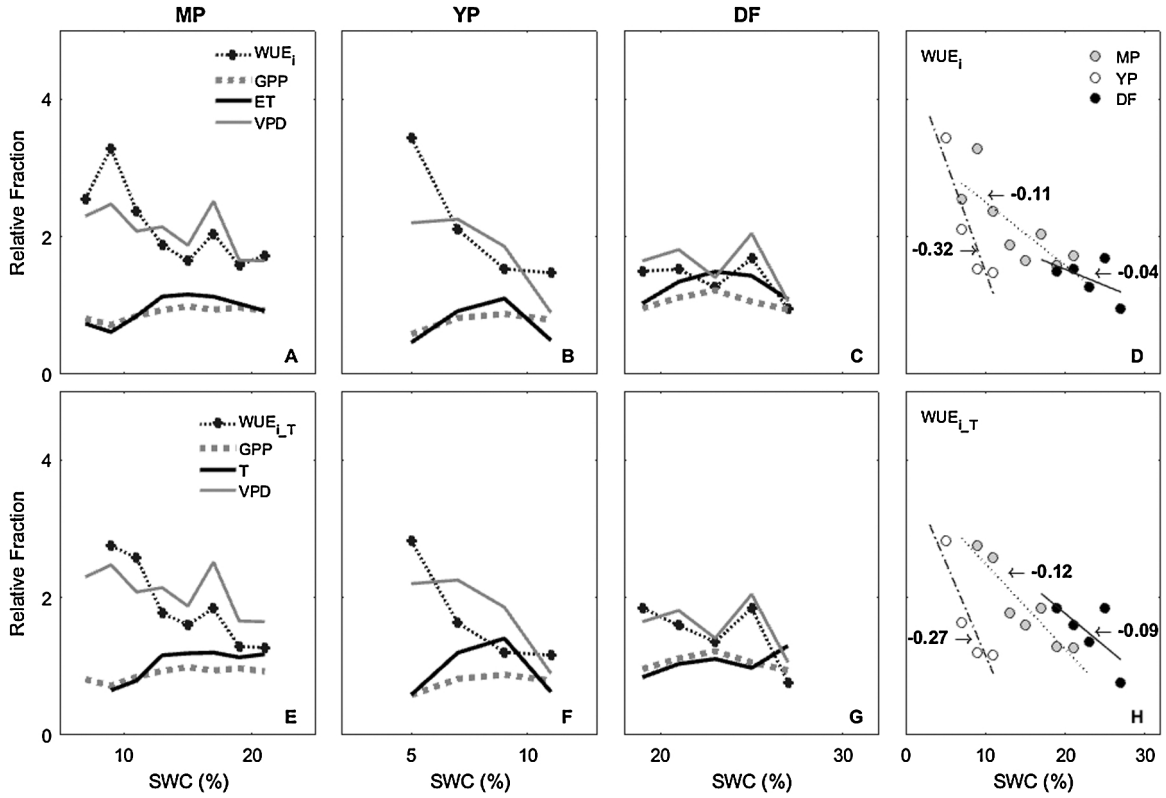

Fig. 4. Relationships between soil water content (SWC) and gross primary productivity (GPP), evapotranspiration (ET), transpiration (T), vapor pressure deficit (VPD), inherent water-use efficiency from ET (WUE_i), and inherent water-use efficiency from T (WUE_{i_T}) during summers for mature ponderosa pine (MP, panels A and E), young ponderosa pine (YP, panels B and F), and mature Douglas-fir (DF, panels C and G). Each variable is presented as a fraction relative to pre-drought conditions. The relationship between SWC and WUE_i for each site (panel D) are described by the following linear regressions: $y = -0.11\,x + 3.71$, $R^2 = 0.68$ at MP, $y = -0.32\,x + 4.72$, $R^2 = 0.52$ at YP, and $y = -0.04\,x + 2.32$, $R^2 = 0.38$ at DF. The relationship between SWC and WUE_{i_T} for each site (panel H) are: $y = -0.12\,x + 3.50$, $R^2 = 0.79$ at MP, $y = -0.27\,x + 3.88$, $R^2 = 0.30$ at YP, and $y = -0.09\,x + 3.69$, $R^2 = 0.56$ at DF. Values next to the regression lines represent the slope of the regression.

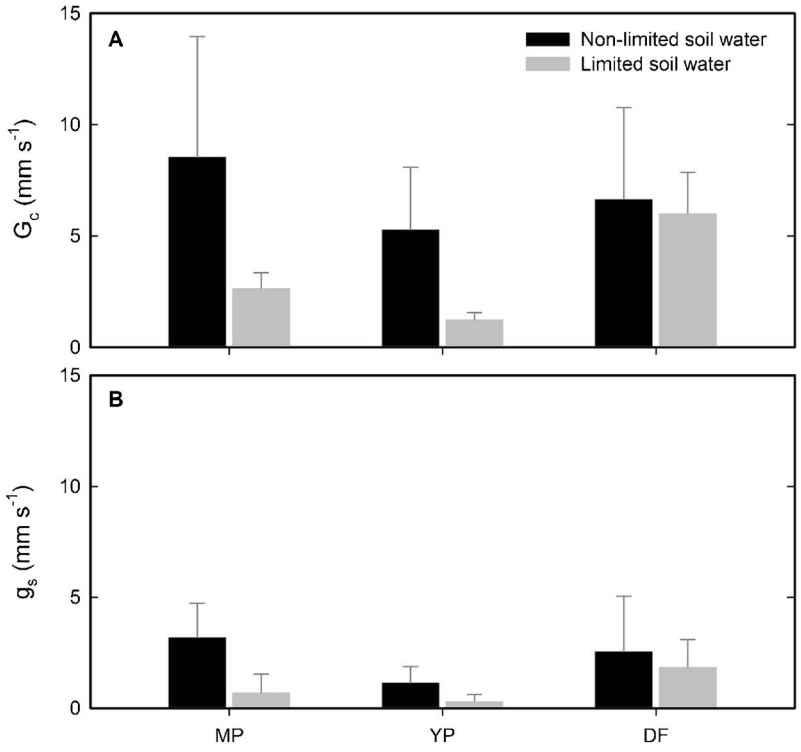

Fig. 5. Values of (A) canopy conductance (G_c) and (B) stomatal conductance (g_s) under non-limited and limited soil water conditions at mature ponderosa pine (MP), young ponderosa pine (YP), and mature Douglas-fir (DF) sites. Daytime data (PAR > 500 μmol m^{-2} s^{-1}) were selected in the analysis from the data collected during the measurement years. Error bar indicates standard deviation.

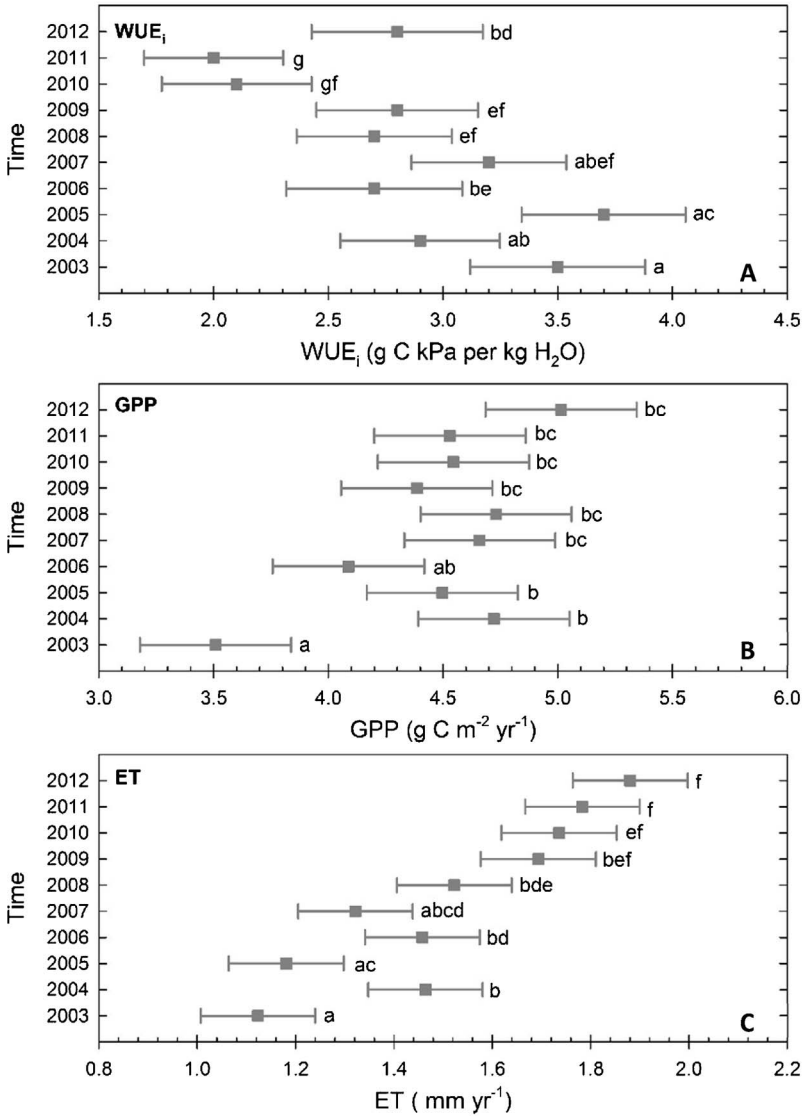

Fig. 6. Variations within the annual means of (A) inherent water-use efficiency (WUE_i), (B) gross primary productivity (GPP), and (C) evapotranspiration (ET) with confidence intervals for each year at the mature ponderosa pine (MP) site. Different letters indicate significant differences between annual values of a given variable ($p < 0.05$).

0.13 g C kPa per kg H_2O per year ($p < 0.05$; Fig. 7A). A positive trend in the ET anomaly (ΔET) was observed (29 mm yr^{-1} with $p < 0.001$), whereas the GPP anomaly (ΔGPP) showed absence of an annual trend (slope of 26 g C yr^{-1} with $p = 0.21$), suggesting ΔWUE_i was more strongly affected by changes in ΔET and not the changes in ΔGPP.

The dependence of annual WUE_i on the timing and quantity of precipitation was assessed by comparing two drought years with different precipitation distributions: a wetter summer in 2004 (58 mm of precipitation over 15 rain events between August and September) and a drier summer in 2005 (< 2 mm with one rain event between August and September, Fig. 8). Compared to the average WUE_i (6.6 g C kPa per kg H_2O) in the two months over the 10-year period, WUE_i decreased by 30% in 2004 (4.4 g C kPa per kg H_2O) and increased by 42% in 2005 (9.3 g C kPa per kg H_2O). WUE_i in 2004 was only half that of in 2005 in these months that showed the most contrasting precipitation patterns. There were more periods of a higher ratio (T/ET) in 2004 when compared to the prolonged dry period in 2005, resulting in a lower WUE_{i_T} in 2004 than 2005. In 2005, prolonged dryness led to a decrease in the ratio of T to ET primarily due to an extremely low T (< 0.2 mm) which resulted in a substantial increase in WUE_{i_T} beginning in mid-August. As found in an experiment by Ruehr et al. (2012), the increase in WUE_i after August was because g_s declined more than photosynthesis. The VPD-induced response of g_s was strongly affected by soil water availability, which affected T more than ET.

To examine the prolonged influence of changing seasonal water availability on interannual WUE_i, we carried out a correlation analysis between annual WUE_i and aggregated monthly water balance over the preceding 24 months (Fig. A.4 in Supplementary materials). Annual WUE_i exhibited a strong negative correlation ($-0.9 < r < -0.5$, $p < 0.05$) with water balance in October when summer drought was alleviated by intensive rains as well as in March at the onset of the wet season. However, the influence of these events on the overall water balance was significant only for a short duration (1–2 months). During the summer drought in July and August, a strong positive correlation was found and the effects persisted for up to 5 months ($0.6 < r < 0.9$, $p < 0.05$). We found no evidence that the effects of seasonal drought had an interannual effect on the water balance at the site.

4. Discussion

4.1. Influence of environment on WUE_i and WUE_{i_T} in mature stands

We compared WUE_i and WUE_{i_T} among species within the evergreen plant functional type in mesic (Douglas-fir) and seasonally water-limited (ponderosa pine) ecoregions. The average annual WUE_i in the overlap years of 2007–2010 was nearly identical for the two stands (2.6 and 2.7 g C kPa per kg H_2O for DF and MP respectively; Fig. 1, Table 2). Although no studies were found that specifically measured WUE_i for

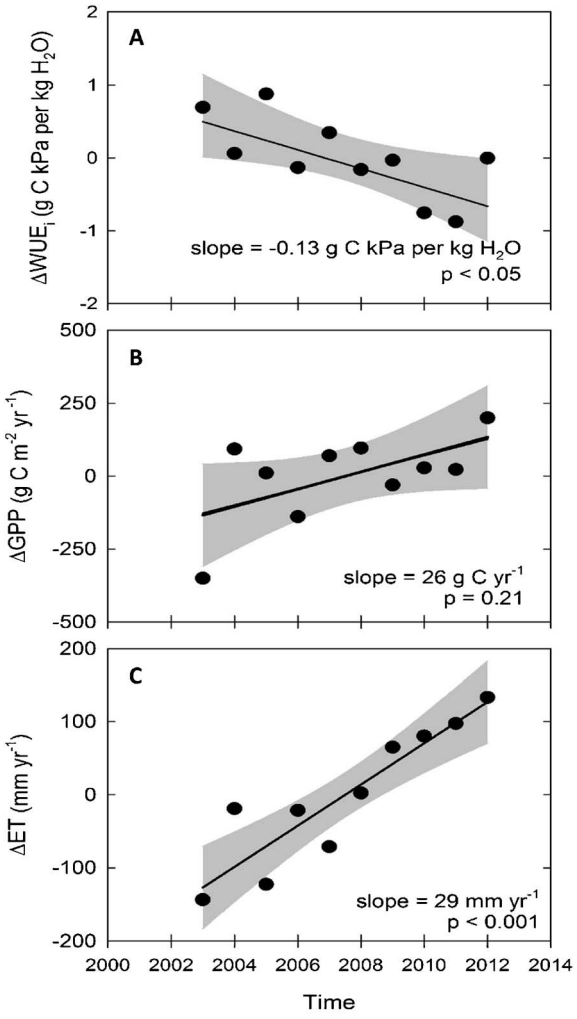

Fig. 7. Trends in the annual anomalies of (A) inherent water-use efficiency (WUE_i), (B) gross primary productivity (GPP), and (C) evapotranspiration (ET) at the mature ponderosa pine (MP) site.

mature ponderosa pine, values for DF and MP were within the range reported by Beer et al. (2009) for evergreen needle-leaved forests which included Douglas-fir, Scots pine, and spruce forests (1.6–3.5 g C kPa per kg H_2O). The average annual WUE_{i_T} in the overlap years of 2007–2009 was greater by roughly 4.0 times in MP (6.2 g C kPa per kg H_2O) compared to DF (1.4 g C kPa per kg H_2O; Table 2), suggesting differences in the physiological responses of plant functional types to soil water availability and climate (Fig. 2).

Soil water content and atmospheric demand played critical roles in driving WUE_i and WUE_{i_T} in MP, whereas trends for DF were almost entirely dependent on atmospheric demand (Figs. 2–4). These results indicate that future changes in the magnitude of VPD due to climate warming will have a significant impact on ecosystem water use (Novick et al., 2016). However, because soil water is still a major factor, and is hyperbolically related to ET, even small changes in soil water will also have large effects on ecosystem WUE (Jung et al., 2010). However, our current predictions of how future patterns in precipitation (and therefore soil moisture) will be altered are uncertain (Burke and Brown, 2008). In drier regions, like those included in this study, soil moisture reserves are depleted rapidly during the summer growing season which have a significant effect on canopy and stomatal conductance (and thus WUE_i and WUE_{i_T}) in these ecosystems (Hubbard et al., 2010) and may be exacerbated by future changes in climate.

The higher sensitivity of WUE_i and WUE_{i_T} to changes in soil water content that were observed in MP can be explained by a larger reduction in both canopy, G_c, and stomatal, g_s, conductance when compared to DF (Fig. 5). Ponderosa pine is more vulnerable to cavitation than Douglas-fir but is considered more drought tolerant (Minore, 1979). Ponderosa pine offsets this vulnerability through functional (more sensitive stomatal closure) and structural (increased sapwood) drought avoidance mechanisms (Stout and Sala, 2003). The pine exhibits greater stomatal sensitivity to stress because of the increased susceptibility of roots to cavitation, which, as drought stress occurs, limits water transport and quickly signals stomatal closure (Alder et al., 1996). Ponderosa pine also shifts biomass allocation from needles to sapwood, thereby increasing water storage and maximizing leaf-area-based water transport even under stress (DeLucia et al., 2000). This adaptation results in the lower GPP and decreased levels of ET that were observed in this study (Fig. 4). Rates of ET decline were greater than those of GPP reduction at both sites and ET decreased more in MP (2.7–0.9 mm d^{-1}) than DF (2.2–1.6 mm d^{-1}) likely reflecting the physiological adaptations of pine to drought. In addition, the contribution of T to ET lessened with soil water depletion, changing from 40 to 30% in MP and from 62 to 40% in DF (data not shown). Lower ratios of T to ET suggest that, under drought stress, changes in ET were mostly due to changes in E, which compensated for the reduced contribution of T from plants to total ecosystem water loss at both sites (Fig. 2).

Humphreys et al. (2003) reported that Douglas-fir showed a higher decline in canopy conductance under very low SWC (< 10%) than under high SWC at a given VPD. In our study, however, higher stomatal closure occurred only on individually isolated hot days (data not shown), which corresponded with high daily maximum water demand that could cause supply velocities through the xylem to become limiting in late summer (VPD > 1.2 kPa; 4% of the total data within the 4-year measurement period). In addition to a relatively higher minimum SWC (20%; Fig. A.2 in Supplementary materials) compared to the sites in Humphreys et al. (2003), sporadic rain events ranging from 2 to 12 days per month in summer caused a transient partial recovery of SWC, leading lesser degree of drought stress to soil water deficit in our sites.

4.2. Influence of stand age on WUE_i and WUE_{i_T}

We found that young and mature pines responded differently to water limitations. The effect of drought stress on WUE_i was more pronounced in young pine than mature pine (Fig. 4D). More severe drought stress in young pine may be due to a lower baseline in soil water content, lesser stem capacitance, and a shallower rooting depth when compared to mature pine. Irvine et al. (2004) reported that a young ponderosa pine extracted 80% of water from a depth of 80 cm or less, whereas a mature ponderosa pine extracted 50% from below 80 cm during summer months. We speculate that shallow root depth at the YP site limited an access to water in deeper soil layers, resulting in lower G_c (1.3 mm s^{-1}; Fig. 5A) and higher sensitivity of WUE_i (Fig. 4D) to soil water content at that site. In addition, the relatively lower LAI at the YP site could result in a higher ratio of E to T during non-limited water periods due the increased amounts of radiation reaching the soil surface. When drought occurs, rates of E may be lowered significantly yielding a much higher value of WUE_i (Vickers et al., 2012).

When WUE_{i_T} was examined as an indicator of whole plant responses to drought at the two pine sites, WUE_{i_T} was 27.2 g C kPa per kg H_2O at the young pine and 10.0 g C kPa per kg H_2O at the mature pine under soil water limited conditions, which were 2.8 and 1.7 times larger than WUE_i, respectively. The higher values of WUE_{i_T} observed in young pine were the result of increased stomatal down-regulation coupled with substantially lowered rates of T (Figs. 2, 4, and 5; Irvine et al., 2004; Law et al., 2000). At the tree level, g_s alters T in order to minimize loss of hydraulic system function (Brooks et al., 2002). Young ponderosa pine have lower hydraulic resistance than mature ponderosa pine, resulting in hydraulic system failure through xylem cavitation and

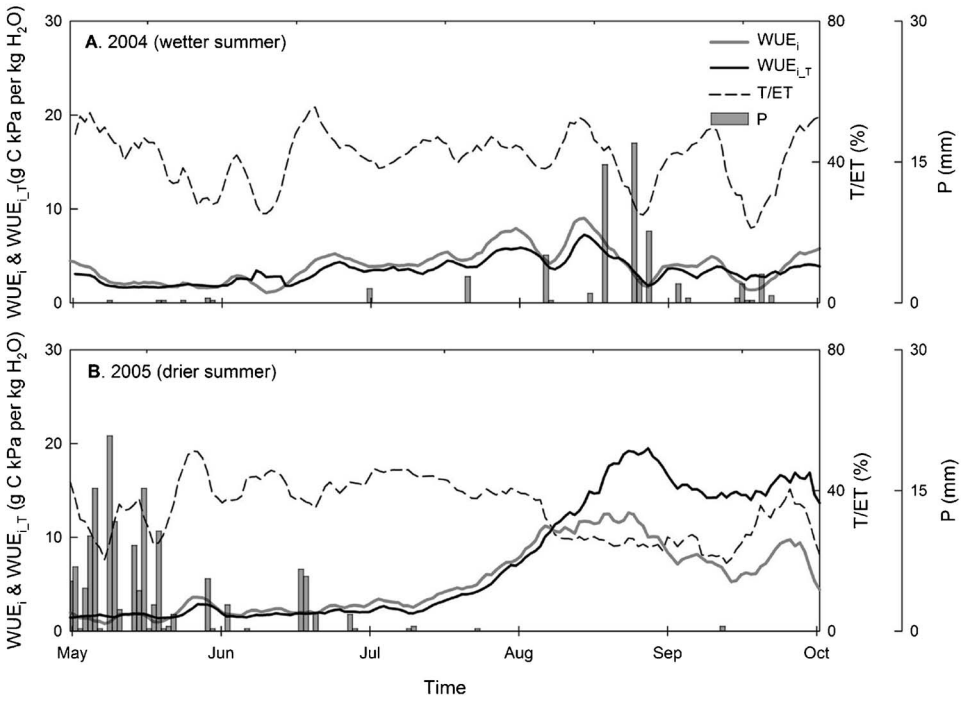

Fig. 8. Comparison of seasonal variation of daily inherent water use efficiency (WUE_i) calculated with evapotranspiration (ET), daily inherent water use efficiency (WUE_{i_T}) calculated with transpiration (T), the ratio of T to ET (T/ET), and precipitation (P) between (A) 2004 (wetter summer) and (B) 2005 (drier summer) at the mature ponderosa pine (MP) site. Seven-day running mean data were used for WUE_i, WUE_{i_T}, and T/ET.

greater restriction in g_s during severe drought periods (Law et al., 2000). In this study, as soil water deficit increased in late summer, values of g_s at the YP site were less than half those observed at the MP (0.3 and 0.7 mm s^{-1} for YP and MP, respectively; Fig. 4B) as a result of lower T rates (0.3 and 0.5 mm d^{-1} for YP and MP, respectively; data not shown).

4.3. Influence of interannual variation in precipitation on mature pine WUE_i

The variation in annual WUE_i in mature ponderosa pine was tightly linked with annual amounts and timing of precipitation. The measurement period at the MP site began with three extremely dry years (2003–2005) and ended with two wet years (2011–2012) which had a significant effect on ET and contributed to the observed decline in ΔWUE_i (-0.13 g C kPa per kg H_2O; Fig. 7). Keenan et al. (2013) found the opposite (an increasing trend of ΔWUE_i with the slope of 0.10 g C kPa per kg H_2O) in mesic temperate and boreal forests of the Northern Hemisphere, which they attributed to rising atmospheric CO_2 that led to increases in photosynthesis and decreasing ET. However, the observed decline in ΔWUE_i in our study was more closely related to the increasing trend in ΔET than any changes in ΔGPP (Fig. 7). Our results suggest that the driving force behind patterns of WUE_i in drought-prone mature ponderosa pine in the Pacific Northwest differs from those reported for other, more mesic, forest ecosystems in global syntheses. This highlights the importance of considering not only the influence of climate variability on local and regional scales but also site/stand characteristics (such as LAI) and species physiology when predicting ecosystem responses to global change (Fig. 2; Beer et al., 2009; Yang et al., 2016).

Despite the strong dependence of annual WUE_i on annual precipitation, we found that precipitation pulses of sufficient magnitude in dry summer months can significantly reduce annual WUE_i (Figs. 6 and 8). Ponderosa pine reacts quickly and dynamically to water availability and even small changes can cause increases in root conductivity and stomatal conductance (Domec et al., 2004). This adaptation led to the increased levels of T as well as lower WUE_i and WUE_{i_T} that were observed in response to the summer precipitation pulses in 2004 (Fig. 8).

Although the seasonality in water availability is the primary driver of annual WUE_i, we did not observe any precipitation legacy, defined as the impact of past precipitation on current ecosystem function, at this site as the temporal imposition of water limitation on annual WUE_i was relieved by the start of wet seasons (winter and spring). Within a given year, drought tended to influence annual WUE_i to a longer extent than that of non-drought (up to 5 months *vs.* up to 2 months, Fig. A.4 in Supplementary materials). The apparent lack of prolonged drought effects could be due to the conservative resource allocation strategy adopted by ponderosa pines in this region, which allots more reserves toward the development of belowground structures for accessing soil water than other species (Williams et al., 2001). This tactic buffers summer droughts and optimizes water use to account for interannual variability in precipitation, which results in relatively stable levels of GPP (Fig. 6B).

5. Conclusion

We investigated climatic and hydrologic effects on WUE_i and WUE_{i_T} across climates and stand ages of the predominant forest types (young and mature ponderosa pines and mature Douglas-fir) in the Pacific Northwest. WUE_i increased with increasing water deficit in the semi-arid young and mature ponderosa pine sites and increasing atmospheric dryness in the mesic Douglas-fir site due to climate variability between locations. Although changes in WUE_i were dependent on soil water content in both young and mature pines, the similar values of WUE_i in young and mature ponderosa pines under non-water limited conditions seems to suggest that WUE_i can be used as a species-specific trait when water availability is high. However, during drought conditions, the mature pine, with its well-established root system, larger stem capacitance, and higher soil water holding capacity, appeared to be better buffered from the effects of seasonal drought. A lower sensitivity of WUE_{i_T} confirmed the lesser influence of seasonal drought on the mature pine than on the young pine. These results emphasize that, even among trees of the same species, individuals of different ages can have markedly different trends in WUE_i and WUE_{i_T} (particularly under drought conditions) and must be incorporated separately into models. Within the evergreen needle-leave plant functional type, Douglas-fir and ponderosa pine are different enough that sub-plant functional type classes, such as genera, would be a reasonable classification for land system modeling (Law, 2014). Therefore, it is of great importance to

take into account both species- and age-specific values of WUE_i and WUE_{i_T} when developing vegetation models for use in predicting forest responses to drought. In addition to ecophysiological influences on WUE_i, understanding the role of T in ecosystem water loss is crucial for the construction of accurate vegetation models. WUE_i can largely be determined by soil physical processes and ET from understory (e.g., 26% of total ET in spring and 20% in summer at mature ponderosa pine) during drought in open canopy forests but the response of the trees can be masked. For a more precise representation of tree drought sensitivity, a transpiration-specific WUE should be utilized in global change modeling.

In the PNW, the effects of drought and forest developmental stage interact to alter carbon and water exchange across the landscape. The semi-arid portion of the PNW region is projected to experience warmer winters and relatively drier summers in the future (Dai, 2013; Dalton et al., 2013). Precipitation is predicted to change by about 10% in the region from 2030 to 2059 (Mote and Salathé, 2010), which could exacerbate drought conditions in already drought-prone areas. The PNW region experienced severe drought in 2015 and the frequency of these types of events are projected to increase in the near future (Wise, 2016). We are just beginning to have a long enough data record to understand ecosystem responses to drought in the major PNW forest types. Identifying drivers of WUE_i variability in seasonally water-limited ecosystems encompassing different drought severities over the long-term may help to predict the responses of carbon and water dynamics to climate change in biomes likely to experience similar conditions in the future.

Acknowledgements

This research was supported by the U.S. Department of Energy's Office of Science (Grant No. DE-FG02-06ER64318 and DE-AC02-05CH11231 for this AmeriFlux core site). We gratefully acknowledge Whitney Creason, Chad Hanson, Dean Vickers, James Irvine, and Andres Schmidt for their field work and valuable comments. We also thank the two reviewers for their helpful comments.

Appendix A. Supplementary data

Supplementary data associated with this article can be found, in the online version, at http://dx.doi.org/10.1016/j.agrformet.2017.08.006.

References

Alder, N.N., Sperry, J.S., Pockman, W.T., 1996. Root and stem xylem embolism, stomatal conductance, and leaf turgor in Acer grandidentatum populations along a soil moisture gradient. Oecologia 105, 293–301.

Allen, C.D., Macalady, A.K., Chenchouni, H., Bachelet, D., McDowell, N., Vennetier, M., Kitzberger, T., Rigling, A., Breshears, D.D., Hogg, E.H., Gonzalez, P., Fensham, R., Zhang, Z., Castro, J., Demidova, N., Lim, J.H., Allard, G., Running, S.W., Semerci, A., Cobb, N., 2010. A global overview of drought and heat-induced tree mortality reveals emerging climate change risks for forests. For. Ecol. Manage. 259, 660–684. http://dx.doi.org/10.1016/j.foreco.2009.09.001.

Assal, T.J., Anderson, P.J., Sibold, J., 2016. Spatial and temporal trends of drought effects in a heterogeneous semi-arid forest ecosystem. For. Ecol. Manage. 365, 137–151. http://dx.doi.org/10.1016/j.foreco.2016.01.017.

Beer, C., Ciais, P., Reichstein, M., Baldocchi, D., Law, B.E., Papale, D., Soussana, J.F., Ammann, C., Buchmann, N., Frank, D., Gianelle, D., Janssens, I.A., Knohl, A., Köstner, B., Moors, E., Roupsard, O., Verbeeck, H., Vesala, T., Williams, C.A., Wohlfahrt, G., 2009. Temporal and among-site variability of inherent water use efficiency at the ecosystem level. Glob. Biogeochem. Cycles 23, GB2018. http://dx.doi.org/10.1029/2008GB003233.

Beguería, S., Vicente-Serrano, S.M., 2013. SPEI: Calculation of the Standardised Precipitation-Evapotranspiration Index.

Black, T.A., Kelliher, F.M., 1989. Processes controlling understorey evapotranspiration. Philos. Trans. R. Soc. Lond. B 324, 207–231.

Brümmer, C., Black, T.A., Jassal, R.S., Grant, N.J., Spittlehouse, D.L., Chen, B., Nesic, Z., Amiro, B.D., Arain, M.A., Barr, A.G., Bourque, C.P.-A., Coursolle, C., Dunn, A.L., Flanagan, L.B., Humphreys, E.R., Lafleur, P.M., Margolis, H.A., McCaughey, J.H., Wofsy, S.C., 2012. How climate and vegetation type influence evapotranspiration and water use efficiency in Canadian forest, peatland and grassland ecosystems. Agric. For. Meteorol. 153, 14–30. http://dx.doi.org/10.1016/j.agrformet.2011.04.008.

Brooks, J.R., Meinzer, F.C., Coulombe, R., Gregg, J., 2002. Hydraulic redistribution of soil water during summer drought in two contrasting Pacific Northwest coniferous forests. Tree Physiol. 22, 1107–1117. http://dx.doi.org/10.1093/treephys/22.15-16.1107.

Burke, E.J., Brown, S.J., 2008. Evaluating uncertainties in the projection of future drought. J. Hydrometeorol. 9, 292–299. http://dx.doi.org/10.1175/2007JHM929.1.

Burnham, K.P., Anderson, D.R., 1998. Model Selection and Multimodel Inference: A Practical Information-Theoretic Approach, 2nd ed. Springer.

Dai, A.G., 2013. Increasing drought under global warming in observations and models. Nat. Clim. Change 3, 52–58. http://dx.doi.org/10.1038/nclimate1633.

Climate Change in the Northwest: Implications for Our Landscapes, Waters, and Communities. In: Dalton, M.M., Mote, P.W., Snover, A.K. (Eds.), Island Press, Washington D.C. http://dx.doi.org/10.5822/978-1-61091-512-0.

DeLucia, E.H., Maherali, H., Carey, E.V., 2000. Climate-driven changes in biomass allocation in pines. Glob. Change Biol. 6, 587–593.

Domec, J.C., Warren, J.M., Meinzer, F.C., Brooks, J.R., Coulombe, R., 2004. Native root xylem embolism and stomatal closure in stands of Douglas-fir and ponderosa pine: mitigation by hydraulic redistribution. Oecologia 141, 7–16. http://dx.doi.org/10.1007/s00442-004-1621-4.

Falge, E., Baldocchi, D., Olson, R., Anthoni, P., Aubinet, M., Bernhofer, C., Burba, G., Ceulemans, R., Clement, R., Dolman, H., Granier, A., Gross, P., Grünwald, T., Hollinger, D., Jensen, N., Katul, G., Keronen, P., Kowalski, A., Ta, C., Law, B.E., Meyers, T., Moncrieff, J., Moors, E., Munger, J.W., Pilegaard, K., Rannik, Ü., Rebmann, C., Suyker, A., Tenhunen, J., Tu, K., Verma, S., Vesala, T., Wilson, K., Wofsy, S., 2001. Gap filling strategies for defensible annual sums of net ecosystem exchange. Agric. For. Meteorol. 107, 43–69.

Foken, T., Wichura, B., 1996. Tools for quality assessment of surface-based flux measurements. Agric. For. Meteorol. 78, 83–105. http://dx.doi.org/10.1016/0168-1923(95)02248-1.

Granier, A., 1987. Evaluation of transpiration in a Douglas-fir stand by means of sap flow measurements. Tree Physiol. 3, 309–320. http://dx.doi.org/10.1093/treephys/3.4.309.

Huang, M., Piao, S., Sun, Y., Ciais, P., Cheng, L., Mao, J., Poulter, B., Shi, X., Zeng, Z., Wang, Y., 2015. Change in terrestrial ecosystem water-use efficiency over the last three decades. Glob. Change Biol. 21, 2366–2378. http://dx.doi.org/10.1111/gcb.12873.

Hubbard, R.M., Stape, J., Ryan, M.G., Almeida, A.C., Rojas, J., 2010. Effects of irrigation on water use and water use efficiency in two fast growing Eucalyptus plantations. For. Ecol. Manage. 259, 1714–1721. http://dx.doi.org/10.1016/j.foreco.2009.10.028.

Humphreys, E.R., Black, T.A., Ethier, G.J., Drewitt, G.B., Spittlehouse, D.L., Jork, E.M., Nesic, Z., Livingston, N.J., 2003. Annual and seasonal variability of sensible and latent heat fluxes above a coastal Douglas-fir forest, British Columbia, Canada. Agric. For. Meteorol. 115, 109–125. http://dx.doi.org/10.1016/S0168-1923(02)00171-5.

IPCC, 1995. The Science of Climate Change, the IPCC Scientific Assessment. Cambridge University Press.

Irvine, J., Law, B.E., Anthoni, P.M., Meinzer, F.C., 2002. Water limitations to carbon exchange in old-growth and young ponderosa pine stands. Tree Physiol. 22, 189–196. http://dx.doi.org/10.1093/treephys/22.2-3.189.

Irvine, J., Law, B.E., Kurpius, M.R., Anthoni, P.M., Moore, D., Schwarz, P.A., 2004. Age-related changes in ecosystem structure and function and effects on water and carbon exchange in ponderosa pine. Tree Physiol. 24, 753–763. http://dx.doi.org/10.1093/treephys/24.7.753.

Irvine, J., Law, B.E., Martin, J.G., Vickers, D., 2008. Interannual variation in soil CO2 efflux and the response of root respiration to climate and canopy gas exchange in mature ponderosa pine. Glob. Change Biol. 14, 2848–2859. http://dx.doi.org/10.1111/j.1365-2486.2008.01682.x.

Jasechko, S., Sharp, Z.D., Gibson, J.J., Birks, S.J., Yi, Y., Fawcett, P.J., 2013. Terrestrial water fluxes dominated by transpiration. Nature 496, 347–350. http://dx.doi.org/10.1038/nature11983.

Jung, M., Reichstein, M., Ciais, P., Seneviratne, S.I., Sheffield, J., Goulden, M.L., Bonan, G., Cescatti, A., Chen, J., de Jeu, R., Dolman, a J., Eugster, W., Gerten, D., Gianelle, D., Gobron, N., Heinke, J., Kimball, J., Law, B.E., Montagnani, L., Mu, Q., Mueller, B., Oleson, K., Papale, D., Richardson, A.D., Roupsard, O., Running, S., Tomelleri, E., Viovy, N., Weber, U., Williams, C., Wood, E., Zaehle, S., Zhang, K., 2010. Recent decline in the global land evapotranspiration trend due to limited moisture supply. Nature 467, 951–954. http://dx.doi.org/10.1038/nature09396.

Keenan, T.F., Hollinger, D.Y., Bohrer, G., Dragoni, D., Munger, J.W., Schmid, H.P., Richardson, A.D., 2013. Increase in forest water-use efficiency as atmospheric carbon dioxide concentrations rise. Nature 499, 324–327. http://dx.doi.org/10.1038/nature12291.

Kim, J., Verma, S., 1990. Components of surface energy balance in a temperate grassland ecosystem. Bound. Layer Meteorol. 51, 401–417. http://dx.doi.org/10.1007/BF00119676.

Lal, R., 2004. Carbon sequestration in dryland ecosystems. Environ. Manage. 33, 528–544. http://dx.doi.org/10.1007/s00267-003-9110-9.

Law, B.E., Williams, M., Anthoni, P.M., Baldocchi, D.D., Unsworth, M.H., 2000. Measuring and modelling seasonal variation of carbon dioxide and water vapour exchange of a Pinus ponderosa forest subject to soil water deficit. Glob. Change Biol. 6, 613–630. http://dx.doi.org/10.1046/J.1365-2486.200000339.X.

Law, B.E., 2014.. Regional analysis of drought and heat impacts on forests: current and future science directions. Glob. Change Biol. 20, 3595–3599. http://dx.doi.org/10.1111/gcb.12651.

Leuzinger, S., Thomas, R., 2011. How do we improve Earth system models? Integrating Earth system models, ecosystem models, experiments and long-term data. New Phytol. 191, 15–18. http://dx.doi.org/10.1111/j.1469-8137.2011.03778.x.

Linderson, M.L., Mikkelsen, T.N., Ibrom, A., Lindroth, A., Ro-Poulsen, H., Pilegaard, K.,

2012.. Up-scaling of water use efficiency from leaf to canopy as based on leaf gas exchange relationships and the modeled in-canopy light distribution. Agric. For. Meteorol. 152, 201–211. http://dx.doi.org/10.1016/j.agrformet.2011.09.019.
Lu, X., Zhuang, Q., 2010. Evaluating evapotranspiration and water-use efficiency of terrestrial ecosystems in the conterminous United States using MODIS and AmeriFlux data. Remote Sens. Environ. 114, 1924–1939. http://dx.doi.org/10.1016/j.rse.2010.04.001.
Lumley, T., 2017. Thomas Lumley Based on Fortran Code by Alan Miller (2017). Leaps: Regression Subset Selection. R Package Version 3.0.
Meddens, A.J.H., Hicke, J.A., Ferguson, C.A., 2012. Spatiotemporal patterns of observed bark beetle caused mortality in British Columbia and the western United States. Ecol. Appl. 22, 1876–1891. http://dx.doi.org/10.1890/11-1785.1.
Minore, D., 1979. Comparative Autecological Characteristics of Northwestern Tree Species – A Literature Review. Gen. Tech. Rep. PNW-87. U. S. Department of Agriculture, Forest Service, Pacific Northwest Forest and Range Experiment Station, Portland, OR.
Mote, P.W., Salathé, E.P., 2010. Future climate in the Pacific Northwest. Clim. Change 102, 29–50. http://dx.doi.org/10.1007/s10584-010-9848-z.
Novick, K.A., Ficklin, D.L., Stoy, P.C., Williams, C.A., Bohrer, G., Oishi, A.C., Papuga, S.A., Blanken, P.D., Noormets, A., Sulman, B.N., Scott, R.L., Wang, L., Phillips, R.P., 2016. The increasing importance of atmospheric demand for ecosystem water and carbon fluxes. Nat. Clim. Change 6, 1023–1027. http://dx.doi.org/10.1038/NCLIMATE3114.
Pan, Y., Birdsey, R., Fang, J., Houhton, R., Kauppi, P., Kurz, W., Phillips, O., Ahvidenko, A., Lewis, S., Canadell, J., Ciais, P., Jackson, R., Pacala, S., McGuire, D., Pia, S., Rautiainen, A., Sitch, S., Hayes, D., 2011. A large and persistent carbon sink in the world's forest. Science 988, 988–993. http://dx.doi.org/10.1126/science.1201609.
Priestley, C.H.B., Taylor, R.J., 1972. On the assessment of surface heat flux and evaporation using large-scale parameters. Mon. Weather Rev. 100, 81–92.
R Core Team, 2016. R: A Language and Environment for Statistical Computing.
Rotenberg, E., Yakir, D., 2010. Contribution of semi-arid forests to the climate system. Science 327, 451–454. http://dx.doi.org/10.1126/science.1179998.
Ruehr, N.K., Martin, J.G., Law, B.E., 2012. Effects of water availability on carbon and water exchange in a young ponderosa pine forest: above- and belowground responses. Agric. For. Meteorol. 164, 136–148. http://dx.doi.org/10.1016/j.agrformet.2012.05.015.
Schwalm, C.R., Williams, C.A., Schaefer, K., Anderson, R., Arain, M.A., Baker, I., Barr, A., Black, T.A., Chen, G., Chen, J.M., Ciais, P., Davis, K.J., Desai, A., Dietze, M., Dragoni, D., Fischer, M.L., Flanagan, L.B., Grant, R., Gu, L., Hollinger, D., Izaurralde, R.C., Kucharik, C., Lafleur, P., Law, B.E., Li, L., Li, Z., Liu, S., Lokupitiya, E., Luo, Y., Ma, S., Margolis, H., Matamala, R., McCaughey, H., Monson, R.K., Oechel, W.C., Peng, C., Poulter, B., Price, D.T., Riciutto, D.M., Riley, W., Sahoo, A.K., Sprintsin, M., Sun, J., Tian, H., Tonitto, C., Verbeeck, H., Verma, S.B., 2010. A model-data intercomparison of CO_2 exchange across North America: results from the North American carbon program site synthesis. J. Geophys. Res. Biogeosci. 115. http://dx.doi.org/10.1029/2009JG001229.
Schwarz, P.A., Law, B.E., Williams, M., Irvine, J., Kurpius, M., Moore, D., 2004. Climatic versus biotic constraints on carbon and water fluxes in seasonally drought-affected ponderosa pine ecosystems. Glob. Biogeochem. Cycles 18. http://dx.doi.org/10.1029/2004gb002234GB4007.
Sellers, P.J., Dickinson, R.E., Randall, D.A., Bets, A.K., Hall, F.G., Berry, J.A., Collatz, G.J., Denning, A.S., Mooney, H.A., Nobre, C.A., Sato, N., Field, C.B., Henderson-Sellers, A., 1997. Modeling the exchanges of energy, water, and carbon between continents and the atmosphere. Science 275, 502–509. http://dx.doi.org/10.1126/science.275.5299.502.
Stout, D.L., Sala, A., 2003. Xylem vulnerability to cavitation in Pseudotsuga menziesii and Pinus ponderosa from contrasting habitats. Tree Physiol. 23, 43–50.
Sun, G., Caldwell, P., Noormets, A., McNulty, S.G., Cohen, E., Moore Myers, J., Domec, J.C., Treasure, E., Mu, Q., Xiao, J., John, R., Chen, J., 2011. Upscaling key ecosystem functions across the conterminous United States by a water-centric ecosystem model. J. Geophys. Res. 116, G00J05. http://dx.doi.org/10.1029/2010JG001573.
Tang, X., Li, H., Desai, A.R., Nagy, Z., Luo, J., Kolb, T.E., Olioso, A., Xu, X., Yao, L., Kutsch, W., Pilegaard, K., Köstner, B., Ammann, C., 2014. How is water-use efficiency of terrestrial ecosystems distributed and changing on Earth? Sci. Rep. 1–11. http://dx.doi.org/10.1038/srep07483.
Tans, P.P., Fung, I.Y., Takahashi, T., 1990. Observational constraints on the global atmospheric CO2 budget. Science 247, 1431–1438.
Thom, A.S., 1972. Momentum, mass and heat exchange of vegetation. Q. J. R. Meteorol. Soc. 98, 124–134. http://dx.doi.org/10.1002/qj.49709841510.
Thomas, C.K., Foken, T., 2002. Re-evaluation of integral turbulence characteristics and their parameterisations. In: 15th Conference on Turbulence and Boundary Layers. Wageningen, NL. pp. 129–132.
Thomas, C.K., Law, B.E., Irvine, J., Martin, J.G., Pettijohn, J.C., Davis, K.J., 2009. Seasonal hydrology explains interannual and seasonal variation in carbon and water exchange in a semiarid mature ponderosa pine forest in central Oregon. J. Geophys. Res. 114, G04006. http://dx.doi.org/10.1029/2009JG001010.
Thomas, C.K., Martin, J.G., Law, B.E., Davis, K., 2013. Toward biologically meaningful net carbon exchange estimates for tall, dense canopies: multi-level eddy covariance observations and canopy coupling regimes in a mature Douglas-fir forest in Oregon. Agric. For. Meteorol. 173, 14–27. http://dx.doi.org/10.1016/j.agrformet.2013.01.001.
Tian, H., Chen, G., Liu, M., Zhang, C., Sun, G., Lu, C., Xu, X., Ren, W., Pan, S., Chappelka, A., 2010. Model estimates of net primary productivity, evapotranspiration, and water use efficiency in the terrestrial ecosystems of the southern United States during 1895–2007. For. Ecol. Manage. 259, 1311–1327. http://dx.doi.org/10.1016/j.foreco.2009.10.009.
U.S. Geological Survey, 1991. National Water Summar 1988–89 Hydrologic Events and Floods and Droughts. U.S. Geological Survey, Water-Supply Paper 2375, Reston, VA.
Vicente-Serrano, S.M., Beguería, S., López-Moreno, J.I., 2010. A multiscalar drought index sensitive to global warming: the standardized precipitation evapotranspiration index. J. Clim. 23, 1696–1718. http://dx.doi.org/10.1175/2009JCLI2909.1.
Vicente-Serrano, S.M., Gouveia, C., Camarero, J.J., Beguería, S., Trigo, R., López-Moreno, J.I., Azorín-Molina, C., Pasho, E., Lorenzo-Lacruz, J., Revuelto, J., Morán-Tejeda, E., Sanchez-Lorenzo, A., 2013. Response of vegetation to drought time-scales across global land biomes. Proc. Natl. Acad. Sci. U. S. A. 110, 52–57. http://dx.doi.org/10.1073/pnas.1207068110.
Vickers, D., Thomas, C.K., Pettijohn, C., Martin, J.G., Law, B.E., 2012. Five years of carbon fluxes and inherent water-use efficiency at two semi-arid pine forests with different disturbance histories. Tellus B 64, 1–14. http://dx.doi.org/10.3402/tellusb.v64i0.17159.
Webb, E.K., Pearman, G.I., Leuning, R., 1980. Correction of flux measurements for density effects due to heat and water vapour transfer. Q. J. R. Meteorol. Soc. 106, 85–100. http://dx.doi.org/10.1002/qj.49710644707.
Williams, M., Law, B.E., Anthoni, P.M., Unsworth, M.H., 2001. Use of a simulation model and ecosystem flux data to examine carbon-water interactions in ponderosa pine. Tree Physiol. 21, 287–298. http://dx.doi.org/10.1093/treephys/21.5.287.
Williams, P.A., Allen, C.D., Macalady, A.K., Griffin, D., Woodhouse, C.A., Meko, D.M., Swetnam, T.W., Rauscher, S. a., Seager, R., Grissino-Mayer, H.D., Dean, J.S., Cook, E.R., Gangodagamage, C., Cai, M., McDowell, N.G., 2012. Temperature as a potent driver of regional forest drought stress and tree mortality. Nat. Clim. Change 3, 292–297. http://dx.doi.org/10.1038/nclimate1693.
Wise, E.K., 2016. Five centuries of U.S. West Coast drought: occurrence, spatial distribution, and associated atmospheric circulation patterns. Geophys. Res. Lett. Res. 43, 4539–4546. http://dx.doi.org/10.1002/2016GL068487.
Yang, Y., Guan, H., Batelaan, O., Mcvicar, T.R., Long, D., Piao, S., Liang, W., Liu, B., Jin, Z., Simmons, C.T., 2016. Contrasting responses of water use efficiency to drought across global terrestrial ecosystems. Sci. Rep. 6, 23284. http://dx.doi.org/10.1038/srep23284.
Zeppel, M.J.B., Adams, H.D., Anderegg, W.R.L., 2011. Mechanistic causes of tree drought mortality: recent results, unresolved questions and future research needs. New Phytol. 192, 800–803. http://dx.doi.org/10.1111/j.1469-8137.2011.03960.x.
Zha, T., Barr, A.G., van der Kamp, G., Black, T.A., McCaughey, J.H., Flanagan, L.B., 2010. Interannual variation of evapotranspiration from forest and grassland ecosystems in western canada in relation to drought. Agric. For. Meteorol. 150, 1476–1484. http://dx.doi.org/10.1016/j.agrformet.2010.08.003.
Zhao, M., Running, S.W., 2010. Drought-Induced reduction in global terrestrial net primary production from 2000 through 2009. Science 329, 940–943. http://dx.doi.org/10.1126/science.1192666.